J Appl Biomater Funct Mater 2015; 13(2): e94-e101
DOI: 10.5301/JABFM.5000186

ORIGINAL ARTICLE

Open Access

Short-term effects of microstructured surfaces: role in cell differentiation toward a contractile phenotype

Francesca Boccafoschi[1], Marco Rasponi[2], Martina Ramella[1], Ana Marina Ferreira[3], Simone Vesentini[2], Mario Cannas[1]

[1]Department of Health Sciences, University of Piemonte Orientale "A. Avogadro," Novara - Italy
[2]Department of Electronics, Information and Bioengineering, Politecnico di Milano, Milano - Italy
[3]Department of Mechanics, Politecnico di Torino, Torino - Italy

S. Vesentini and M. Cannas contributed equally to this work.

ABSTRACT

Cell adhesion plays a key role in cell behavior, in terms of migration, proliferation, differentiation and apoptosis. All of these events concur with tissue regeneration and remodeling mechanisms, integrating a complex network of intracellular signaling modules. Morphogenetic responses, which involve changes in cell shape, proliferation and differentiation, are thought to be controlled by both biochemical and biophysical cues. Indeed, the extracellular matrix not only displays adhesive ligands necessary for cell adhesion but also plays an essential biomechanical role – responsible, for instance, for the acquisition of the contractile phenotype. The substrate topography around the forming tissues and the associated mechanical stresses that are generated regulate cellular morphology, proliferation and differentiation. Thus, the ability to tailor topographical features around cells can be a crucial design parameter in tissue engineering applications, inducing cells to exhibit the required performances.

In this work, we designed micropillared substrates using highly spaced arrays (interspacing equal to 25 μm) to evaluate the effects of topography on C2C12 myoblasts' adhesion and differentiation. Optical and fluorescence microscopy images were used to observe cell adhesion, together with Western blot analysis on vinculin and focal adhesion kinase (FAK) expression, a protein highly involved in adhesive processes. Differentiation marker (Myf5, myogenin and myosin heavy chain [MHC]) expression was also studied, in relation to the effect of different substrate topographies on the enhancement of a contractile phenotype. Our results demonstrated that microstructured surfaces may play a key role in the regeneration of functional tissues.

Key words: C2C12 differentiation, Cell adhesion, Microscale topography, Myf5, Myogenin, Myosin heavy chain, Vinculin

Accepted: November 20, 2013

INTRODUCTION

Cells in the body adhere to the surrounding extracellular matrix (ECM), and this condition is primarily related to cell survival. At this level, surface integrins are responsible not only for the physical attachment of cells to the matrix, but also for sensing and transducing mechanical signals from focal adhesion sites to the cytoskeletal machinery (1). During this process, known as mechanotransduction, various physical cues in a cell's surrounding environment are converted to biochemical, intracellular signaling responses that lead to changes in cell function (2, 3). Indeed, these signals are known to drive various cellular processes that include migration (4, 5), proliferation (6), differentiation (7) and apoptosis (8). In particular, adherent cells exert strong traction forces at their sites of anchorage to the ECM, depending on the size of the focal contacts (9).

In vivo, the ECM, through its structure and molecular composition, presents a variety of geometrically defined, 3-dimensional (3D) physical cues at micron and submicron levels (10-12). In contrast, cells in vitro face bioartificial surfaces, which represent their primary source of physical stimuli. By understanding the manner in which cells interact with their physical environment, it may be possible to control cellular behavior through the fabrication

of substrates with specific physical properties. For this purpose, nanofabrication and microfabrication technologies have being widely used to construct substrates of differing topographies. In this regard, microfabrication techniques have been used to affect supracellular behavior and to develop inexpensive and scalable features (13). Moreover, biologists and bioengineers have taken advantage of microtopography to induce and study specific cell behaviors (14-18). Cell morphology and adhesion have been studied on several types of topographies, including grooves (19), pillars (20, 21), wells (22), pits (23) and pyramidal-shaped microstructures (24). The capability of microfabrication techniques in generating various topographical stimuli mimicking the native cell microenvironment's architecture has provided valuable insights about the relationship between the cell–substrate interaction and cellular processes. All of these events concur with tissue remodeling mechanisms, integrating a complex network of intracellular signaling modules. For example, in cases of injuries, an organized cascade of events is induced to favor the expression of suitable phenotypes and restore the original functionalities of tissues. However, several cell processes are still unknown, and a better understanding of cell behavior promoted by microstructured substrates promises to speed up the discovery of adequate solutions to restoring tissue functionality.

In the case of contractile tissues (i.e., skeletal muscles, myocardium and blood vessels), 2 factors are essential for the development of synthetic substrates able to functionally regenerate the surrounding tissues: adequate cell adhesion and suitable substrate elasticity to induce and maintain the cellular differentiation toward a particular contractile phenotype (25).

The molecular complexity of the processes which lead to cell adhesion includes membrane and cytoskeletal proteins involved in the formation of focal contacts (e.g., vinculin) as well as signaling molecules tightly associated with several intracellular pathways (e.g., Rho GTPases) (26). Focal adhesions are multiprotein complexes able to connect the ECM with the cytoskeletal stress fibers, through specific transmembrane proteins (integrins) tightly connected in the inner membrane with an adhesion plaque formed by roughly 50 different proteins. The adhesion plaque is also connected with the cytoskeleton and with related cytoskeletal pathways (27).

In this study, we aimed at investigating the collective effect of microstructured topographies on the behavior of C2C12 skeletal myoblasts. Two rounded micropillar patterns were fabricated on polydimethylsiloxane (PDMS) substrates, yielding different effective substrate elasticities. Our results demonstrated that microstructured surfaces help to enhance cell adhesion, promoting cell differentiation toward a contractile phenotype. Thus, our results confirmed that surface topography may play a key role at a supracellular level in the regeneration of functional tissues.

MATERIALS AND METHODS

Fabrication of microstructured substrates

In this study, 2 patterned microstructured surfaces were considered for cell culture experiments. Both patterns consisted of arrays of pillars with identical nominal diameter (6 μm) and center-to-center distance (spacing equal to 25 μm), but different heights. The nominal height of pillars of substrate A (short pillars) was set to roughly 4 μm, while pillars of substrate B had a height of 10 μm (tall pillars).

Mold fabrication

Substrates were fabricated by replica molding of polydimethylsiloxane (PDMS; Dow Corning, Midland, MI, USA). The molds were made on silicone wafers by standard photolithography using a positive photoresist (AZ4562; Microchemicals GmbH, Germany), deposited up to the desired thickness for both configurations. After development, resist was reflown on a hotplate at 250°C for 30 minutes to achieve round-shaped posts. The final molds were then cast by pouring fresh PDMS onto the wafer molds, cured at 70°C for 3 hours, peeled off, and silanized to aid subsequent releases. The steps of the process are depicted in Figure 1.

Cell culture substrates

For both mold configurations, fresh PDMS in the ratio 10:1 was finally used to cast the cell culture substrates directly onto the silicone molds. Each pillar array had external dimensions of 10×10 mm. Flat PDMS substrates were also cast and used as control.

Characterization of topographies

Scanning electron microscopy (SEM) images were acquired for both micropillar substrates, and used to measure the resulting specific dimensions using ImageJ software (Image Processing and Analysis in Java version 1.45, available on http://rsb.info.nih.gov/nih-image/).

To assess substrate stiffness, individual pillar geometries were considered. When a load (F) is applied on the top of the pillar, a deflection δ is produced, which is the function of the inverse of the product of the material's Young's modulus by the second moment of inertia (I) (which is the only function of the pillar geometry). According to Ghibaudo et al (28), the spring constant (k) of a single cylindrical micropillar can be directly obtained from the material's elastic modulus (E) and pillar's geometry (through the second moment of inertia) by applying the Euler-Bernoulli beam theory. The shape of pillar tested in the present work – that is, the ellipsoid –

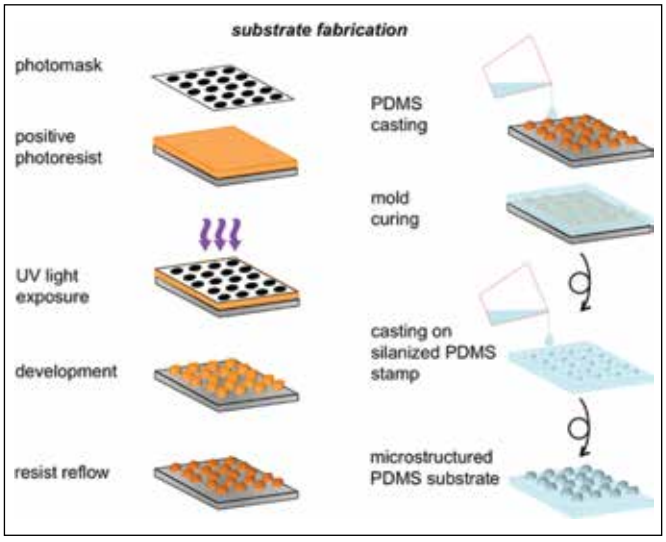

Fig. 1 - *Procedures used to fabricate microstructured substrates: positive photoresist was spun on silicon wafers to the desired thickness; upon development, resist was reflown on a hotplate to provide posts with a ellipsoidal shape; polydimethylsiloxane (PDMS) was then poured on the wafer molds, silanized, and used as final mold. A final PDMS casting enabled the production of the final pillar arrays for cell culture experiments.*

reduces the second moment of inertia by a factor of 9/15 and consequently also the stiffness by the same amount. Finally, the spring constant of a single micropillar can be used to obtain an effective Young's modulus (E_{eff}) of the overall substrate, with 2.5 MPa being the Young's modulus for the bare PDMS (28).

The wettability property of substrates was also assessed by measuring the contact angles through the sessile drop method. Briefly, a drop of bidistilled water (5 µL) was placed on sample substrates, and the angle formed by the water drop and the surface was observed microscopically and measured at a temperature of 25°C.

Cell culture

C2C12 myoblast cells (ATCC CRL1772; American Type Culture Collection, Rockville, MD, USA) isolated from mouse muscle were cultured in Dulbecco's modified Eagle's medium (DMEM) enriched with 10% fetal bovine serum, glutamine (2 mM), penicillin (100 U/mL) and streptomycin (100 mg/mL) (Euroclone, Milan, Italy). Prior to cell experiments, both micropillar and control substrates were cleaned with ethanol, rinsed with deionized water, coated with fibronectin (10 µg/mL in water) and incubated at 37°C for 1 hour. Cells were then seeded (density of $1x10^4$ cells/cm^2) on fibronectin pre-coated sample surface and maintained at 37°C throughout the entire experiments in a humidified atmosphere with 5% CO_2, and visually inspected after 24 and 72 hours using an optical microscope.

Fluorescent microscopy

Cells were cultured on different surfaces for 72 hours, fixed in phosphate-buffered saline (PBS)–buffered formalin for 30 minutes and then labeled with phalloidin TRITC-conjugated (Sigma, Italy) to visualize actin filaments. 4',6-Diamidino-2-phenylindole dihydrochloride (DAPI) was used for nuclear staining. Cells were observed by fluorescent microscope (Leica, TGS 4D) at a ×40 magnification.

Viability test (MTT assay)

To evaluate cell viability, a 3-(4,5-dimethylthiazol-2-yl)-2,5-diphenyltetrazolium bromide (MTT) assay (CellTiter Aqueous NonRad Cell Prolif Assay; Promega, Italy) was performed. Cells were cultured on different surfaces for 24 and 72 hours. A 3-(4,5-dimethylthiazol-2-yl)-5-(3-carboxymethoxyphenyl)-2-(4-sulfophenyl)-2H-tetrazolium inner salt (MTT) solution was added to culture medium. After 3 hours, culture medium was removed, the formazan salts that had formed were dissolved with dimethyl sulfoxide (DMSO), and the solution was analyzed by UV-VIS spectroscopy (V-630 UV-Vis Spectrophotometer; Jasco, USA) at 570 nm. The absorbance was directly proportional to the number of viable cells.

Western blot analysis

After 72 hours, cells were lysed in boiling sodium dodecyl sulfate (SDS) (1 M Tris-HCl, pH 7.4, 10% SDS, H_2O) (heated up at 95°C for 5 minutes) and sonicated.

Protein concentration was determined with a bicinchoninic acid assay (Pierce, Rockford, IL, USA). Then, 20 µg of total proteins in loading buffer (62.5 mM Tris-HCl, pH 6.8, 20% glycerol, 2% SDS, 5% b-mercaptoethanol, 0.5% bromophenol blue) was used for sodium dodecyl sulfate–polyacrylamide gel electrophoresis (SDS-PAGE) and transferred to a nitrocellulose membrane (Amersham Biosciences, Buckinghamshire, UK).

Blotted proteins were blocked with 5% non-fat dried milk in PBS, pH 7.4, for 1 hour at room temperature and then incubated overnight with primary antibodies (vinculin, FAK, FAK^{Y397}, p21, proliferating cell nuclear antigen [PCNA], Myf5, myogenin, myosin heavy chain [MHC]; all from Millipore, Italy) at a ratio of 1:500 in PBS.

After washing 3 times with PBS 0.1% Tween 20, membranes were incubated with peroxidase-conjugated secondary antibodies (Amersham Biosciences, Buckinghamshire, UK) for 1 hours at room temperature.

After washing 3 times with PBS 0.1% Tween 20, protein bands were visualized using ECL detection reagents (Amersham Biosciences, Buckinghamshire, UK) in a chemosensitive visualizer (VersaDoc, BioRad, Italy). Tests were performed in triplicate for each experimental condition.

Densitometry

A semiquantitative examination was carried out on results obtained from Western blot analyses. The images acquired were analyzed with image analysis software (QuantityOne; Biorad). To take into account optical density and extension of protein bands, these were evaluated on a gray scale index/mm^2 in pixels (optical density).

Statistical analysis

Experiments were performed in triplicate, and results were expressed as means ± standard deviation. Statistical analysis of variance (ANOVA) was used, and the significance of differences between means was assessed by Bonferroni's method, taking P≤0.05 as the minimum level of significance.

RESULTS

Substrate characteristics

SEM images of the micropillar substrates are shown in Fig. 2a, both in top and lateral views. The measured heights were 4±0.2 and 10±0.4 μm for samples A and B, respectively. The diameters of the posts were measured in correspondence of their basis and were found to be 6±0.6 and 7±0.9 μm for samples A and B, respectively. In addition, the surface area of each pillar configuration was calculated and used to evaluate the overall surface area available to cells. For this purpose, pillars were modeled as spherical caps. Table I summarizes the resulting cell culture areas within each micropillar array configuration, together with the geometrical surveys, expressed as means ± standard deviation. Control indicates a flat PDMS surface.

Mechanical stiffness of the micropillar substrates was characterized by their values for E_{eff}, which spanned 1 order of magnitude, ranging from 110 kPa to 1.07 MPa. Table I also reports a comparison between effective elasticities of substrates in the case where pillars had a traditional cylindrical shape versus an ellipsoidal shape, where E_{eff} values are reduced to about 60%.

Due to the chemical composition of PDMS, the wettability of the control surface indicates a weak hydrophobicity (contact angle 100.9±1). The A topography displayed similar characteristics, with a measured contact angle of 95.8±1.1. Instead, substrate B showed an increased, and statistically significantly different, hydrophobic behavior (angle of 107.1±1.1 degrees). Figure 2b shows representative images taken during the contact angle measurements.

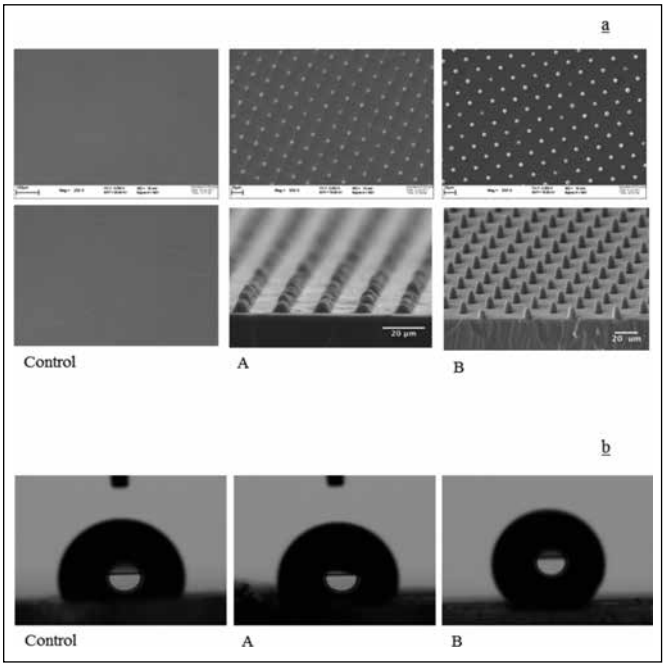

Fig. 2 - ***a)*** *Scanning electron microscopy (SEM) images of control and micropillared surfaces* ***(A, B, C)*** *from top and lateral view.* ***b)*** *Contact angle images showing water drop shapes during the processes. Relative measures are reported in Table I.*

Cell adhesion, proliferation and differentiation

Cell adhesion and proliferation were observed on both control and micropillar substrates after 24 and 72 hours (Fig. 3). At 24 hours, the presence of post arrays seemed not to show any significant differences in terms of adhesion efficiency and cell spreading compared with control. Fluorescence images after 72 hours showed that cells seeded on micropillared surfaces formed continuous monolayers, displaying a substantial spindle shape. Well-formed podosomes (white arrows) were appreciable on all the surfaces, even if quantitatively more present on B samples. Although control was suitable for cell adhesion and growth, the cell monolayer was less defined and cells grew forming several clusters. These results were strengthened by Western blot analyses of vinculin and FAK expression.

Cell viability showed no significant differences after 24 hours of culturing, while it was greatly enhanced on cells seeded on microstructured surfaces at 72 hours (Fig. 4).

Western blot analyses showed a relevant vinculin and FAK expression on cells seeded on both microstructured surfaces, with a significant increase with respect to control (Fig. 5). No statistically significant differences were observed between A and B topographies.

To evaluate the ability of micropillared surfaces to induce switching between proliferating to synthetic states, p21 together with proliferating cell nuclear antigen (PCNA)

TABLE I - MICROPILLAR ARRAY CHARACTERISTICS: AVERAGE PILLAR DIAMETERS (2r) AND HEIGHTS (h) AS MEASURED THROUGH SEM MICROSCOPY AND IMAGEJ SOFTWARE, WITH INTERPILLAR SPACING (s) AS A DESIGN PARAMETER

Substrate configuration	2r [μm]	h [μm]	s [μm]	area [cm²]	E_{eff} cylinder [MPa]	E_{eff} ellipsoid [MPa]	contact angle [°]
Control	-	-	-	1	2.5	2.5	100.9±1
A	6±0.6	4±0.2	25	1.05	1.78	1.07	95.8±1.1
B	7±0.9	10±0.4	25	1.15	0.18	0.11	107.1±1.1

Values are means ± standard deviation. Micropillar array characteristics: average pillar diameters (2r) and heights (h) were measured through SEM microscopy and ImageJ software, while the interpillar spacing (s) was a design parameter. The effective area available to cells was computed through geometrical considerations by assuming pillars as oblate ellipsoids. Similarly, the overall substrate effective elasticity (E_{eff}) was calculated from the ideal case of cylindrical pillars, and scaling by a shape correction factor. The last column contains the contact angles of the micropillared substrates as measured with the sessile drop method and a drop shape analysis system at 25°C.

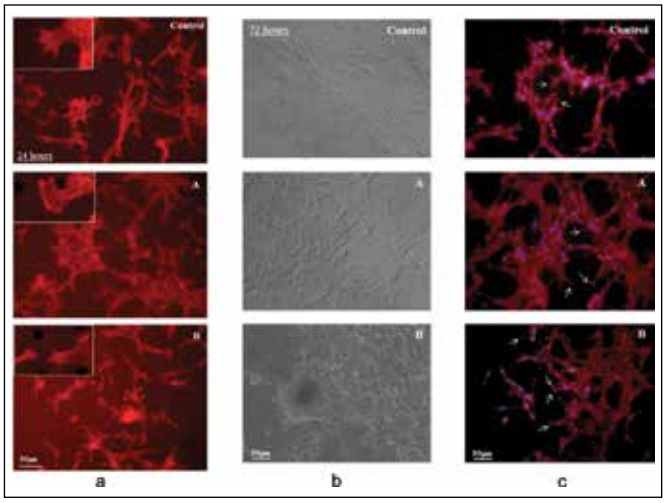

Fig. 3 - ***a)*** *Fluorescent microscopy images of C2C12 seeded on different substrates at 24 hours. A higher magnification has been used to show the cell adhesion on the pillars.* ***b)*** *Micrographs with an optical microscope were collected after 72 hours of culturing, visually showing cell adhesion and proliferation on different substrates.* ***c)*** *Fluorescent microscopy images of C2C12 seeded on different substrates. Rhodamine-phalloidin was used for actin filaments and DAPI for nuclear staining. Cells were observed after 72 hours of seeding. Figures are representative of 3 different experiments.*

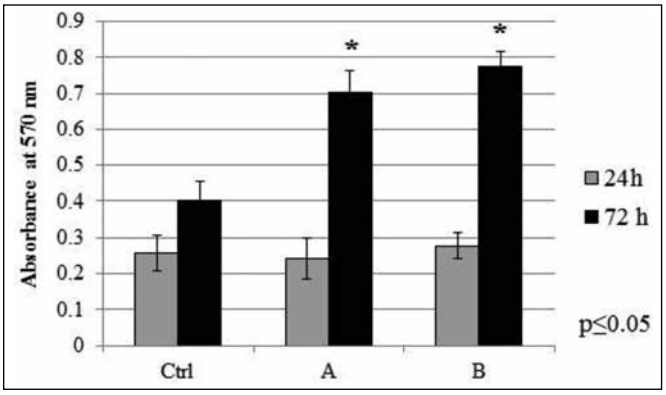

Fig. 4 - *Cell viability at 24 and 72 hours performed using MTT assay. *P≤0.05.*

expression was investigated (Fig. 6). Cells seeded on control surfaces exhibited a down-regulated expression of p21, known as a regulator of cell cycle progression at the G_1/S checkpoint, thus characterizing cells with a proliferative status. In contrast, the presence of microstructured surfaces up-regulated the p21 expression, which was significantly increased, particularly on B topography. PCNA expression was used as an indicator of cell proliferation. Cells seeded on A and B substrates expressed a significantly decreased level of PCNA compared with control.

Finally, to further evaluate the influence of topographical features on the differentiation process toward a contractile phenotype, Myf5, myogenin and MHC expressions were studied and compared (Fig. 7). After 72 hours of culturing, all of the myogenetic markers (Myf5, myogenin and MHC) were significantly up-regulated on micropillared substrates with respect to control. No statistically significant differences were shown between the 2 different substrate morphologies considered.

DISCUSSION

Recent studies have shown different biological responses modulated by surface topography – for instance, using grooving/ridges (29), by grinding the substrates with abrasives (30), by using UV lithography (31, 32).

Using microfabrication and replica molding we generated 2 arrays of ellipsoidal micropillars. The round-shaped pillars were achieved by reflowing positive photoresists on developed wafer molds. Due to this geometry, the effect of topographies did not lead to significant variations to the contact angle with respect to the control (flat PDMS substrate). As previously shown, micropillar arrays are able to modify the nanoscale and microscale mechanics of the substrate, allowing the tuning of its effective elasticity (28). The effect on the mechanics of the modified geometries was a reduction of about 40% in the effective elastic modulus thus representing a valuable complementary procedure in obtaining arrays with tuned rigidity. From a biological standpoint, our data suggest that cell viability and differentiation are regulated depending on rigidity E_{eff}.

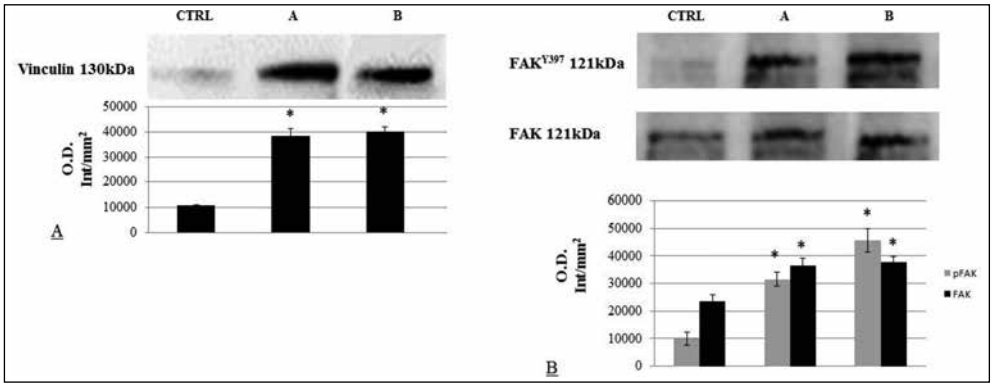

Fig. 5 - *Western blot analysis with anti-vinculin and FAK antibodies on lysates from C2C12 cells cultured for 72 hours on different surfaces. Densitometry graphics obtained from 3 different experiments are expressed as means ± standard deviation. *P≤0.05, vs. control.*

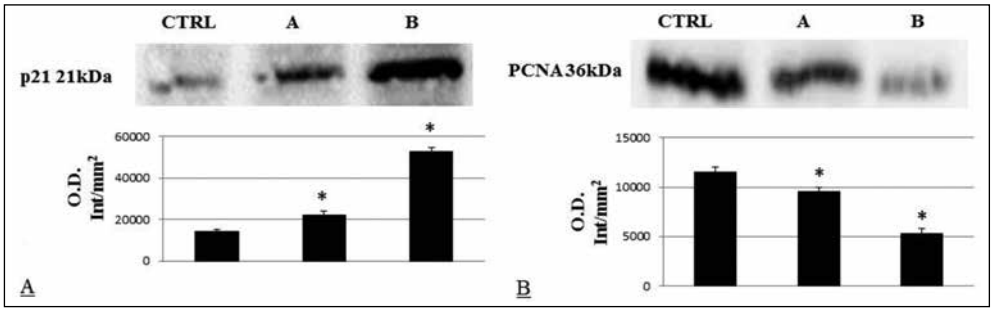

Fig. 6 - *Western blot analyses with anti-p21 and anti-proliferating cell nuclear antigen (anti-PCNA) antibody on lysates from C2C12 cells cultured for 72 hours on different surfaces. Densitometry graphics obtained from three different experiments are expressed as mean ± standard deviation. *P≤0.05, vs. control.*

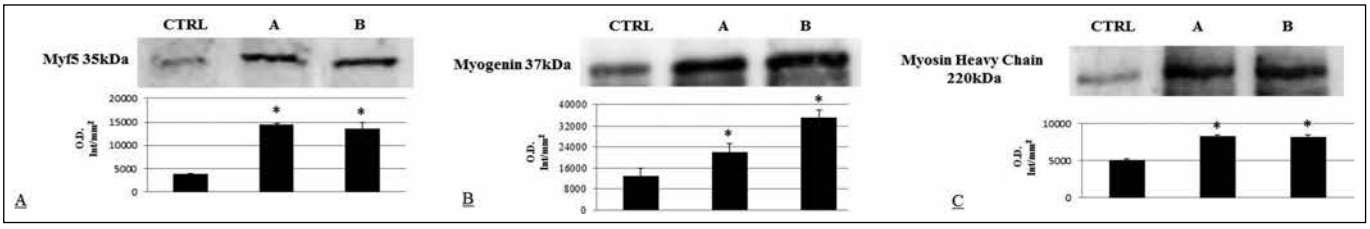

Fig. 7 - *Western blot analysis of anti-Myf5* ***(A)****, anti-myogenin* ***(B)*** *and anti-myosin heavy chain (anti-MHC)* ***(C)*** *antibodies on lysates from C2C12 cells cultured for 72 hours on different surfaces. Densitometry graphics obtained from 3 different experiments are expressed as means ± standard deviation. *P≤0.05, vs. control.*

The first consequence of a microstructured substrate was a significant improvement of cell adhesion stability. In fact, vinculin and FAK, which is a protein involved in focal contact formation, were significantly up-regulated on microstructured surfaces. An increase in focal adhesion size and organization with increasing substrate stiffness has already been observed by Guo and colleagues, together with an increased recruitment of vinculin to adhesive sites on stiffer substrates (33). The morphological observations (fluorescent images) showed the formation of filopodia, particularly remarkable on micropillared substrate, with nicely formed podosomes especially on B substrate. Furthermore, focal contacts are directly related to intracellular molecular pathways, involving the Rho GTPase family. These molecular pathways are responsible for cytoskeletal reorganization, eventually leading to actin polymerization (Rac1), stress fiber formation and smooth muscle contraction (RhoA) (34). Our results (data not shown) clearly showed that surface topography has direct effects not only on focal contact formation, but even on the involvement of the related molecular pathways such as Rho GTPases. Thus, geometrical cues conferred by micropatterns possibly lead to different tensile stresses and cytoskeletal reorganization of C2C12 cells, which ultimately caused different degrees of differentiation on the geometry configuration tested. Moreover, the literature reports that FAK is activated in differentiating C2C12 cells, and Tyr397 phosphorylation is required for fusion of myoblasts in myotubes in the late events of the differentiation process (35). By the way, concerning differentiation, it is very difficult to point out a single molecule that might be responsible for up-regulation of myogenesis on a particular geometry, as there are 32 known molecules that are involved in the mammalian process of myoblast fusion (36). These proteins can be broadly classified into 3 major types: namely, membrane-associated, intracellular and extracellular/secreted molecules. It is well known

that there are 4 known muscle regulatory factors (MRFs) – MyoD, Myf5, myogenin and MRF4 – that are involved in in vitro myogenesis (37, 38). We used Myf5, myogenin and MHC as targets of different stages (early and late) of myogenesis differentiation on substrates with different stiffness. Our results support the hypothesis that cell response greatly depends on substrate rigidity with regards to cell differentiation (39). Indeed, consistent with the work of Discher and coworkers (25), the presence of micropillar structures caused a reduction in terms of substrate effective elasticity (ranging from 1.01 MPa to 110 kPa), determining a significant enhancement of the expression of both myogenesis markers.

CONCLUSIONS

Synthetic substrates may help in tissue engineering as scaffold for regenerative medicine applications. In particular, an adequate substrate should improve cell adhesion and maintenance of cell functionality. This work showed that microstructured surfaces enhance cell adhesion, specifically guiding cell behavior toward a contractile phenotype. These findings should be a valid support for tissue engineering applications, in particular when cell contractility is required. For instance, an interesting field would be represented by muscle tissue, both smooth or skeletal, where the tissue functionality is focused on the cells' ability to contract, avoiding the formation of a scar fibrotic tissue which generally possesses a very low elasticity and an almost absent contractility, both not suitable characteristics to sustain an optimal muscle tissue regeneration. Furthermore, the ability to drive cellular processes through the engineering of substrate topography still requires further studies. For example, to date, analytical models are only able to predict wetting characteristics due to conventional topographies (40). The availability of more sophisticated models will thus represent a key element in the development of optimized substrates for advanced cell culture experiments.

Financial support: This research was partially supported by the Politecnico di Milano grant titled "5 per mille junior" 2009 (CUP: D41J10000490001).

Conflict of interest: None.

Address for correspondence:
Francesca Boccafoschi
Department of Health Sciences
University of Piemonte Orientale "A. Avogadro"
Via Solaroli 17
IT-28100 Novara, Italy
francesca.boccafoschi@med.unipmn.it

REFERENCES

1. Nikkhah M, Edalat F, Manoucheri S, Khademhosseini A. Engineering microscale topographies to control the cell-substrate interface. Biomaterials. 2012; 33(21): 5230-5246.
2. Fletcher DA, Mullins RD. Cell mechanics and the cytoskeleton. Nature. 2010; 463(7280): 485-492.
3. Eyckmans J, Boudou T, Yu X, Chen CS. A hitchhiker's guide to mechanobiology. Dev Cell. 2011; 21(1): 35-47.
4. Galbraith CG, Sheetz MP. Forces on adhesive contacts affect cell function. Curr Opin Cell Biol. 1998; 10(5): 566-571.
5. Burton K, Park JH, Taylor DL. Keratocytes generate traction forces in two phases. Mol Biol Cell. 1999; 10(11): 3745-3769.
6. Chen CS, Mrksich M, Huang S, Whitesides GM, Ingber DE. Geometric control of cell life and death. Science. 1997; 276(5317): 1425-1428.
7. Li B, Lin M, Tang Y, Wang B, Wang JHC. A novel functional assessment of the differentiation of micropatterned muscle cells. J Biomech. 2008; 41(16): 3349-3353.
8. Jean C, Gravelle P, Fournie JJ, Laurent G. Influence of stress on extracellular matrix and integrin biology. Oncogene. 2011; 30(24): 2697-2706.
9. Stricker J, Aratyn-Schaus Y, Oakes PW, Gardel ML. Spatiotemporal constraints on the force-dependent growth of focal adhesions. Biophys J. 2011; 100(12): 2883-2893.
10. Goodman SL, Sims PA, Albrecht RM. Three-dimensional extracellular matrix textured biomaterials. Biomaterials. 1996; 17(21): 2087-2095.
11. Abrams GA, Goodman SL, Nealey PF, Franco M, Murphy CJ. Nanoscale topography of the basement membrane underlying the corneal epithelium of the rhesus macaque. Cell Tissue Res. 2000; 299(1): 39-46.
12. Pamuła E, De Cupere V, Dufrêne YF, Rouxhet PG. Nanoscale organization of adsorbed collagen: influence of substrate hydrophobicity and adsorption time. J Colloid Interface Sci. 2004; 271(1): 80-91.
13. Park TH, Shuler ML. Integration of cell culture and microfabrication technology. Biotechnol Prog. 2003; 19(2): 243-253.
14. Bettinger CJ, Langer R, Borenstein JT. Engineering substrate topography at the micro- and nanoscale to control cell function. Angew Chem Int Ed Engl. 2009; 48(30): 5406-5415.
15. Kim DH, Wong PK, Park J, Levchenko A, Sun Y. Microengineered platforms for cell mechanobiology. Annu Rev Biomed Eng. 2009; 11(1): 203-233.

16. Hoffman-Kim D, Mitchel JA, Bellamkonda RV. Topography, cell response, and nerve regeneration. Annu Rev Biomed Eng. 2010; 12(1): 203-231.
17. le Digabel J, Ghibaudo M, Trichet L, Richert A, Ladoux B. Microfabricated substrates as a tool to study cell mechanotransduction. Med Biol Eng Comput. 2010; 48(10): 965-976.
18. Moraes C, Sun Y, Simmons CA. (Micro)managing the mechanical microenvironment. Integr Biol (Camb). 2011; 3(10): 959-971.
19. Rajnicek A, Britland S, McCaig C. Contact guidance of CNS neurites on grooved quartz: influence of groove dimensions, neuronal age and cell type. J Cell Sci. 1997; 110(Pt 23): 2905-2913.
20. Turner AM, Dowell N, Turner SW, et al. Attachment of astroglial cells to microfabricated pillar arrays of different geometries. J Biomed Mater Res A. 2000; 51(3): 430-441.
21. Ghibaudo M, Trichet L, Le Digabel J, Richert A, Hersen P, Ladoux B. Substrate topography induces a crossover from 2D to 3D behavior in fibroblast migration. Biophys J. 2009; 97(1): 357-368.
22. Wang L, Murthy SK, Fowle WH, Barabino GA, Carrier RL. Influence of micro-well biomimetic topography on intestinal epithelial Caco-2 cell phenotype. Biomaterials. 2009; 30(36):6825-6834.
23. Wan Y, Wang Y, Liu Z, et al. Adhesion and proliferation of OCT-1 osteoblast-like cells on micro- and nano-scale topography structured poly(L-lactide). Biomaterials. 2005; 26(21): 4453-4459.
24. Le Saux G, Magenau A, Böcking T, Gaus K, Gooding JJ. The relative importance of topography and RGD ligand density for endothelial cell adhesion. PLoS ONE. 2011; 6(7): e21869.
25. Discher DE, Mooney DJ, Zandstra PW. Growth factors, matrices, and forces combine and control stem cells. Science. 2009; 324(5935): 1673-1677.
26. Critchley DR. Focal adhesions: the cytoskeletal connection. Curr Opin Cell Biol. 2000; 12(1): 133-139.
27. Cabodi S, del Pilar Camacho-Leal M, Di Stefano P, Defilippi P. Integrin signalling adaptors: not only figurants in the cancer story. Nat Rev Cancer. 2010; 10(12): 858-870.
28. Ghibaudo M, Di Meglio JM, Hersen P, Ladoux B. Mechanics of cell spreading within 3D-micropatterned environments. Lab Chip. 2011; 11(5): 805-812.
29. Wang P-Y, Yu H-T, Tsai W-B. Modulation of alignment and differentiation of skeletal myoblasts by submicron ridges/grooves surface structure. Biotechnol Bioeng. 2010; 106(2): 285-294.
30. Shimizu K, Fujita H, Nagamori E. Micropatterning of single myotubes on a thermoresponsive culture surface using elastic stencil membranes for single-cell analysis. J Biosci Bioeng. 2010; 109(2): 174-178.
31. Patz TM, Doraiswamy A, Narayan RJ, et al. Three-dimensional direct writing of B35 neuronal cells. J Biomed Mater Res B Appl Biomater. 2006; 78(1): 124-130.
32. Charest JL, Jennings JM, King WP, Kowalczyk AP, García AJ. Cadherin-mediated cell-cell contact regulates keratinocyte differentiation. J Invest Dermatol. 2009; 129(3): 564-572.
33. Guo WH, Frey MT, Burnham NA, Wang YL. Substrate rigidity regulates the formation and maintenance of tissues. Biophys J. 2006; 90(6): 2213-2220.
34. Kaibuchi K, Kuroda S, Amano M. Regulation of the cytoskeleton and cell adhesion by the Rho family GTPases in mammalian cells. Annu Rev Biochem. 1999; 68(1): 459-486.
35. Clemente CF, Corat MA, Saad ST, Franchini KG. Differentiation of C2C12 myoblasts is critically regulated by FAK signaling. Am J Physiol Regul Integr Comp Physiol. 2005; 289(3): R862-R870.
36. Jansen KM, Pavlath GK. Molecular control of mammalian myoblast fusion. Methods Mol Biol. 2008; 475: 115-133.
37. Yoshida N, Yoshida S, Koishi K, Masuda K, Nabeshima Y. Cell heterogeneity upon myogenic differentiation: down-regulation of MyoD and Myf-5 generates 'reserve cells'. J Cell Sci. 1998; 111(Pt 6): 769-779.
38. Kitzmann M, Fernandez A. Crosstalk between cell cycle regulators and the myogenic factor MyoD in skeletal myoblasts. Cell Mol Life Sci. 2001; 58(4): 571-579.
39. Nemir S, West JL. Synthetic materials in the study of cell response to substrate rigidity. Ann Biomed Eng. 2010; 38(1): 2-20.
40. Lee JB, Gwon HR, Lee SH, Cho M. Wetting transition characteristics on microstructured hydrophobic surfaces. Mater Trans. 2010; 51(9): 1709-1711.